Applied and Computational Mechanics 5 (2011) 239–252

Possibility of identification of elastic properties in laminate beams with cross-ply laminae stacking sequences

M. Zajíček[a,*], J. Dupal[a]

[a] *Faculty of Applied Sciences, University of West Bohemia, Univerzitní 22, 306 14 Plzeň, Czech Republic*

Received 4 October 2011; received in revised form 23 December 2011

Abstract

The goal of this work is to show the possibility of the identification of laminate beam specimens elastic properties with cross-ply laminae stacking sequences using prescribed eigenfrequencies. These frequencies are not determined experimentally in this paper but they are calculated numerically by means of the finite element (FE) software MSC.Marc. The composite material properties of the FE model based on Euler-Bernoulli theory have been subsequently tuned to correlate the determined frequencies in cross-ply laminate beams with the eigenfrequencies obtained by the software package. A real-coded genetic algorithm (GA) and a micro-genetic algorithm (μGA) are applied as the inverse technique for the identification problem. Because a small efficiency of the GAs in searching for Poisson's ratio values was found, this parameter and the in-plane shear modulus have been estimated by using the law of mixtures. Some numerical examples are given to illustrate the proposed technique.

Keywords: cross-ply laminate, beam, genetic algorithm, inverse technique, finite element model

1. Introduction

Composite materials are widely employed in modern industry. Analysis and design of structures manufactured from these materials depend directly upon accurate knowledge of their properties. Hence the property evaluation is one of the important goal of research.

Chu and Rokhlin [5] determined the elastic properties of composite from ultrasonic bulk wave velocity data. Balasubramaniam and Rao [2] carried out the reconstruction of material stiffness properties of unidirectional fiber-reinforced composites especially from incident ultrasonic bulk wave data. Computer-generated ultrasonic phase velocity data were used as the input to the GA that has been implemented for the parameters reconstruction. In the above two references, the Christoffel equation was applied to establish the relationship between material properties and bulk wave velocity. Complicated techniques were needed to measure the phase velocity of ultrasonic bulk waves and only single-ply anisotropic materials were considered in their works.

A number of researchers developed numerical-experimental methods in which experimental eigenfrequencies were used to identify elastic properties of composites. An indirect identification method for prediction the composite properties of plate specimens using measured eigenfrequencies is presented in [18]. The authors applied the Mindlin plate theory in combination with a FE model for the laminate analysis. Frederiksen [6] identified the elastic constants of thick orthotropic plates, whereas a mathematical model based on the higher-order shear deformation theory has been applied. This solution provides reliable estimations of the two transverse

*Corresponding author. Tel.: +420 377 632 328, e-mail: zajicek@kme.zcu.cz.

shear moduli. Ip et al. [10] also investigated eigenfrequencies in the orthotropic material. Furthermore, the mode shapes were measured on specimens with balanced symmetric lamination which were excited by an impact hammer. In parallel, an analytical model describing the modal responses of composite shells was developed using the Rayleigh-Ritz method. This model was subsequently tuned to correlate the theoretical frequencies with the measurements via Bayesian estimation. In the study [19], physical experiments were performed on the sample plates to measure the eigenfrequencies by a real-time television holography. The basic idea of the proposed approach corresponds to simple FE models which are determined only in the reference points of the experiment design. Therefore, a significant reduction against the conventional methods of minimization can be achieved in calculations of the cost function.

Liu et al. [15] developed the hybrid numerical method (HNM) which has been employed to calculate the transient waves in anisotropic laminated plates excited by impact loads. It combines the finite element method (FEM) with the method of Fourier transforms and it is described in [16]. The HNM and its modified version is then used as a forward solver in some identification problems, see e.g. [13, 14]. The GA or μGA, alternatively combined with another method (for example with the nonlinear least squares method [13]), were usually adopted in these works as the inverse operator controlling the forward solver for material characterization using elastic waves. In the work [14], the dynamic displacement responses were obtained at only one receiving point of laminate surfaces. The robustness of procedure of the measurement noise effect has been investigated by adding Gauss noise to the input displacement response. Han et al. [9] utilized HNM to reconstruct the elastic constants of the cross-ply laminated axisymmetric cylinders subjected to an impact load. In this case, the laminated cylinder was divided into layered cylindrical elements in the thickness direction.

In addition, other techniques of material properties identification have been introduced in recent years. For instance, Genovese et al. [7] published a novel hybrid procedure for the mechanical characterization of orthotropic materials. This identification reverse problem has been solved by combining spectral interferometry and a combinatorial optimization technique, known as simulated annealing. Another numerical-experimental method for the identification of orthotropic materials is given in [12]. A biaxial tensile test was performed on a cruciform test specimen. The displacement field observed by a CCD camera and measured by a digital image correlation technique has been compared with a strain field which was computed by FEM. Newton-Raphson algorithm was used as an optimisation procedure. Kam and Liu [11] presented method for the determination of bending stiffness distribution of laminated shafts. The difference between predicted and measured deflections was minimized at any two points on the shaft using a quasi-Newton method. The view of material properties identification techniques is covered by Chen and Kam [4] who developed a two-level optimization method for material characterization by using two symmetric angle-ply beams with different fiber angles subjected to three-point bending. The best estimates of shear modulus and Poisson's ratio of the beam with fiber angles 45° are determined in the first-level optimization process. In the second level, the known shear modulus and Poisson's ratio are kept constant and Young's moduli of the second angle-ply beam with fiber angles different from 45° are identified.

In the present study, the possibility of the prediction of elastic properties in laminate beam specimens with different cross-ply laminae stacking sequences using prescribed eigenfrequencies is presented. The frequencies are determined by the FE software package in place of using the experimental method. These values were compared with the spectral analysis results of the FE models of beam. The GA and μGA are applied to manage the inverse problem.

2. FE formula in forward analysis

The FE model of beam based on Euler-Bernoulli theory is used for the calculation of the eigen-frequencies. In the (x_1, x_2, x_3) coordinate system, the displacement field is given by

$$u_1(x_1, x_3, t) = u(x_1, t) + x_3\,\psi(x_1, t)\,, \quad u_2(x_1, x_2, x_3, t) = 0\,, \quad u_3(x_1, t) = w(x_1, t)\,, \quad (1)$$

where $u(x_1, t)$ and $w(x_1, t)$ are the displacements due to extension and bending, respectively, and $\psi(x_1, t)$ denotes rotation about the x_2-axis. Besides, the displacement $u(x_1, t)$ can be re-written in the form

$$u(x_1, t) = u_c(x_1, t) - z_c\psi(x_1, t)\,, \qquad \text{where} \qquad z_c = B_{11}/A_{11}\,. \quad (2)$$

The symbol $u_c(x_1, t)$ denotes the centroidal axis displacement. The stiffness parameters A_{11} and B_{11} are defined as

$$(A_{11}, B_{11}) = \sum_{k=1}^{n} Q_{11}^k \int_{h_{k-1}}^{h_k} b(x_3)(1, x_3)\mathrm{d}x_3\,, \quad (3)$$

where

$$Q_{11}^k = \frac{E_k}{1 - \nu_{LT}\nu_{TL}} \qquad \text{and} \qquad E_k = \begin{cases} E_L & \text{for} \quad \theta_k = 0\,, \\ E_T & \text{for} \quad \theta_k = \pi/2\,. \end{cases} \quad (4)$$

The longitudinal E_L and transverse E_T Young's modulus including the Poisson's ratios ν_{LT}, ν_{TL} represent the material properties of beam FE model that is consisted of n layers which are supposed to be orthotropic in the (L, T, T') directions, see Fig. 1. Each layer k is extended from lower face h_{k-1} to upper face h_k in the x_3 direction. The angle θ_k is orientated with respect to the x_1-axis and takes only values 0 or $\pi/2$. It is also depicted in Fig. 1 that the FE model is symmetric in the $x_1 - x_3$ plane. The beam cross-section is assumed to be uniform with a various shape having width $b(x_3)$ and the overall thickness h. The length of the FE is l_e.

The two-noded elements are used for the beam discretization. The linear and cubic polynomials are chosen as the displacement shape functions of the element, i.e.

$$u_c(x_1, t) = [1, x_1][a_0(t), a_1(t)]^T, \quad w(x_1, t) = \left[1, x_1, x_1^2, x_1^3\right]\left[a_2(t), a_3(t), a_4(t), a_5(t)\right]^T. \quad (5)$$

Consequently, the functions $u(x_1, t)$, $w(x_1, t)$ and $\psi(x_1, t)$ which describe deformations of a beam element can be expressed in terms of the nodal displacement components $\boldsymbol{q}_e(t) = [\boldsymbol{q}_1(t), \boldsymbol{q}_2(t)]^T$, where

$$\boldsymbol{q}_1(t) = [u(0, t), u(l_e, t)]^T \qquad \text{and} \qquad \boldsymbol{q}_2(t) = [w(0, t), w(l_e, t), \psi(0, t), \psi(l_e, t)]^T. \quad (6)$$

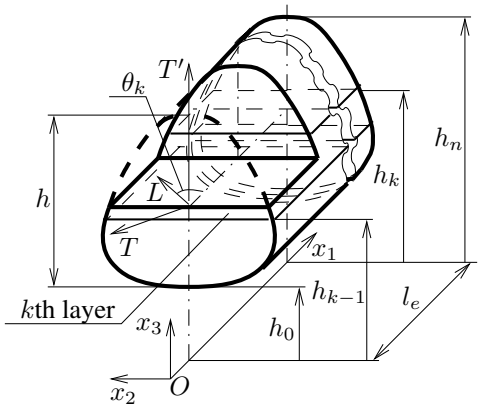

Fig. 1. FE model of laminated beam with symmetric cross-section

Because the derivation of the FE beam is based on Euler-Bernoulli theory, the relation $\psi = -\partial w/\partial x_1$ is valid. Then only one stress tensor component $\sigma_{11} = \sigma_1$ is generally nonzero. Therefore the constitutive equations of the kth layer reduce to

$$\sigma_1^k = Q_{11}^k \, \varepsilon_1 \,, \tag{7}$$

where ε_1 is a strain tensor component ε_{11} and the parameter Q_{11}^k is given by relation (4).

Using the principle of virtual work, the element governing equation of the free vibrations can be written as

$$\boldsymbol{M}_e \ddot{\boldsymbol{q}}_e(t) + \boldsymbol{K}_e \boldsymbol{q}_e(t) = \boldsymbol{0} \,, \tag{8}$$

where $\boldsymbol{M}_e$ and $\boldsymbol{K}_e$ are element mass matrix and element stiffness matrix, respectively. The detail form of these matrices is stated in [22] where the viscoelastic orthotropic beam element was derived according to Timoshenko theory. However, the FE beam based on Euler-Bernoulli theory can be easily obtained by omitting the transverse shear strain as it is mentioned in that paper. Assembling all the element matrices, the free vibration equation of the beam can be expressed in the form

$$\boldsymbol{M} \ddot{\boldsymbol{q}}(t) + \boldsymbol{K} \boldsymbol{q}(t) = \boldsymbol{0} \,, \tag{9}$$

where $\boldsymbol{M}$ is the total mass matrix, $\boldsymbol{K}$ is the total stiffness matrix and $\boldsymbol{q}$ is the global nodal displacement vector. When the periodic motion is considered, i.e. $\boldsymbol{q} = \boldsymbol{\nu} \, \mathrm{e}^{\mathrm{i}\,\Omega\, t}$, Eq. (9) can be rewritten as

$$(\boldsymbol{K} - \Omega^2 \boldsymbol{M}) \boldsymbol{\nu} = \boldsymbol{0} \,, \tag{10}$$

whose solution leads to eigenvalue problem. The symbols $\boldsymbol{\nu}$ and Ω denote eigenvector and eigenfrequency, respectively. It could be found in [22] that the matrix $\boldsymbol{M}$ depends only on the material density and the beam geometry provided that Euler-Bernoulli theory has been considered. Therefore, the new eigenfrequencies can be obtained by solving Eq. (10) when the matrix $\boldsymbol{K}$ is updated with different elastic material constants. The eigenfrequencies calculated from Eq. (10) are then taken as an input for the inverse analysis.

3. Inverse problem formulation

The main aim of inverse methods is the determination of a selected set of unknown parameters in a numerical model. It is necessary to define the objective function which has to be minimized in the feasible domain of optimization parameters. In our case, this function is constructed using the sum of relative difference squares of the components of two vectors containing eigenfrequencies. Then the parametric optimization problem could be formulated as follows:

$$\widehat{\boldsymbol{p}} = \arg \left\{ f_o(\widehat{\boldsymbol{p}}) = \min_{\boldsymbol{p} \in \mathcal{D}} [f(\boldsymbol{p})] = \min_{\boldsymbol{p} \in \mathcal{D}} \left[\sum_{i=1}^{n} (1 - \Omega_i(\boldsymbol{p}) / \Omega_i^{\mathrm{exp}})^2 \right] \right\} , \tag{11}$$

where $\boldsymbol{p} = [\alpha_1, \ldots, \alpha_s]^T \in \mathcal{D} \subseteq \boldsymbol{R}^s$ is a vector of unknown optimization parameters. The domain $\mathcal{D}$ is a convex set and is defined by constraints: $\alpha_k^l \leq \alpha_k \leq \alpha_k^u$ for $k = 1, 2, \ldots, s$. The vector $\boldsymbol{\Omega}^{\mathrm{exp}} = [\Omega_1^{\mathrm{exp}}, \ldots, \Omega_n^{\mathrm{exp}}]^T$ represents eigenfrequencies that are considered as known. Finally, $\boldsymbol{\Omega}(\boldsymbol{p}) \in \boldsymbol{R}^n$ is the vector of eigenfrequencies which are computed from Eq. (10) for admissible values of a vector $\boldsymbol{p}$. The GAs are then employed to search these unknown parameters α_k. The main procedure of the GAs for our problem is presented below.

4. Genetic algorithms

These are very effective algorithms searching for optimal or near-optimal solutions over the investigated finite domain. These methods have been developed by Goldberg [8] according to the idea of Darwin's Theory of Evolution. The GAs are suitable for finding the global optimum of optimization problems which have many local maxima and minima. They also posses the advantages of easy solving of the mixed problems with continuous and discrete variables, and without need of the objective function continuity. For these reasons, the GAs have been adopted to our optimization problem (11).

In the traditional GA, all variables of interest are encoded as binary digits which are known as genes. Collection of these genes further forms so-called chromosome. After manipulation of a binary-coded GA, the final binary numbers are then decoded as original real numbers. On the other hand, a real-coded GA has been also proposed in recent years, see e.g. [3]. The main discrepancy is that all genes in a chromosome are real numbers. It is more convenient to deal with most practical engineering applications because the changes from a real number to the binary digits may be the cause of a loss of the number precision. A real-coding also promotes the calculation efficiency because of straightforward using numbers in representation. Moreover, the various types of genetic operations can be simply adjusted or defined, as given in [17]. For these reasons the real-coded GAs are used in this paper to estimate the elastic properties in laminate beams with cross-ply laminae stacking sequences. In addition to the above, it should be mentioned that attempts to utilize the combination of binary and real genes to identify the unknown system can be found in literature. For example, a hybrid GA taking the advantage of binary and real digits including quantum computing is presented in [21].

In this work, the GA making use of the traditional genetic operators is applied as optimization technique. The algorithm starts with an initial population of N chromosomes randomly selected in the searching space $\mathcal{D}$. The selection, crossover and mutation operations are consequently performed to create next generation. The elitism operator is also adopted to replicate the best individual of current generation. This process is repeated until the convergence criterion or the maximum generation number N_g is achieved.

It has been pointed out in previous studies that a μGA is more robust algorithm for solving multi-parameter inverse problems than the traditional GA. According to Liu and Xi [16], the robustness of a uniform μGA lies in producing of a new genetic information due to the population restart process. Therefore, the μGA has been as well used besides the GA to search the unknown parameters. The structure of this algorithm is a similar to the above described GA but some differences can be found. The population is very small and usually includes only 5 or 6 individuals. Due to this fact, small discrepancies among individuals in the population are observed in a few generations and the convergence to some optimum occurs. At this point, a new population is randomly generated while keeping the best individual from the previously converged generation and the evolution process is thus restarted. The mutation operator is not applied for the population evaluation in the μGA because of new chromosomes keep flowing when the micro population is reborn.

Before the brief description of used real-coded genetic operations, some notations should be introduced. Let the vector of unknown parameters $\boldsymbol{p}_i = [\alpha_{1i}, \ldots, \alpha_{si}]^T$, see Eq. (11), means the ith chromosome in the gth generation of a population $P(g) = \{\boldsymbol{p}_1, \ldots, \boldsymbol{p}_{P_s}\}$ where $i = 1, \ldots, P_s$ while P_s is population size. Furthermore, the parameters p_c and p_m evaluate a probability of the performance of crossover and mutation operations, respectively.

4.1. Selection operation

The tournament selection has been chosen to generate offsprings since it is quite simple and suitable for checking whether a chromosome is reproduced or not according to its corresponding objective function. We randomly select 2 (may be up to $P_s - 1$) individuals from the current population and the best one minimum objective function value is added to the next population which is consequently subjected to other genetic operations. The process is repeated P_s times.

In addition, the roulette wheel selection mechanism is described in this part. This method is utilized below in the selection of suitable crossover type. The roulette wheel selection can be visualized by an imaginary wheel. Each parameter of observed set occupies an area that is related to its objective function value. When a spinning wheel stops, which is in practice represented by a randomly generated number from the range $\langle 0, 1\rangle$, a fixed marker determines selected parameter. Such a selection mechanism needs more numerical computations but the probability of more frequent selection of one parameter can be easily increased, see the next subsection.

4.2. Crossover operation

As mentioned earlier, probability of crossover p_c is one of the parameters of genetic system. This probability gives us the expected number $p_c \times P_s$ of chromosomes which undergo the crossover operation. The process is started by generating a random number r from the range $\langle 0, 1\rangle$ for each chromosome in the population that was subjected to the tournament selection. If $r < p_c$, the chromosome is selected for crossover. These parents are consequently mated randomly to make offsprings, i.e. new chromosomes. The result of this operation significantly depends on selected type of operator. In this work, the three various types of crossover operators are applied in evolutional algorithms. Note that the parameter $a \in (0, 1)$ contained in the following relations is generated randomly.

4.2.1. Simple crossover

Let parents $\boldsymbol{p}_i = [\alpha_{1i}, \ldots, \alpha_{si}]^T$ and $\boldsymbol{p}_j = [\alpha_{1j}, \ldots, \alpha_{sj}]^T$ are selected to be crossed after the kth position where $k \in \{1, 2 \ldots, s-1\}$ is a random number. The offsprings $\tilde{\boldsymbol{p}}_i$ and $\tilde{\boldsymbol{p}}_j$ are then in the form

$$\begin{aligned} \tilde{\boldsymbol{p}}_i &= [\alpha_{1i}, \ldots, \alpha_{ki}, (1-a)\,\alpha_{k+1,i} + a\,\alpha_{k+1,j}, \ldots, (1-a)\,\alpha_{si} + a\,\alpha_{sj}]^T, \\ \tilde{\boldsymbol{p}}_j &= [\alpha_{1j}, \ldots, \alpha_{kj}, (1-a)\,\alpha_{k+1,j} + a\,\alpha_{k+1,i}, \ldots, (1-a)\,\alpha_{sj} + a\,\alpha_{si}]^T. \end{aligned} \tag{12}$$

The results obtained from test cases in [17] showed that the system without simple crossover is less stable than the system without arithmetical crossover. In these tests, the traditional GA has been used in solving of optimization problems.

4.2.2. Arithmetical crossover

This operator is defined as a linear combination of two vectors. If parents $\boldsymbol{p}_i$ and $\boldsymbol{p}_j$ are crossed, the offsprings are given as follows:

$$\tilde{\boldsymbol{p}}_i = a\,\boldsymbol{p}_i + (1-a)\,\boldsymbol{p}_j\,, \qquad \tilde{\boldsymbol{p}}_j = a\,\boldsymbol{p}_j + (1-a)\,\boldsymbol{p}_i\,. \tag{13}$$

It follows from tests performed by Michalewicz [17] that the GA without arithmetical crossover has slower convergence.

4.2.3. Heuristic crossover

This operator is unique because it utilizes values of the objective function $f(\boldsymbol{p})$ defined in Eq. (11) to the determination of next search direction. Moreover, the heuristic crossover produces only a single offspring. Regarding to this fact, we generate the parameter a twice for the given parents $\boldsymbol{p}_i$ and $\boldsymbol{p}_j$, and the following process of determination of a chromosome $\tilde{\boldsymbol{p}}$ is also repeated two times,

$$\tilde{\boldsymbol{p}} = \begin{cases} \boldsymbol{p}_j + a\,(\boldsymbol{p}_j - \boldsymbol{p}_i) & \text{for} \quad f(\boldsymbol{p}_j) \leq f(\boldsymbol{p}_i)\,, \\ \boldsymbol{p}_i + a\,(\boldsymbol{p}_i - \boldsymbol{p}_j) & \text{otherwise.} \end{cases} \tag{14}$$

It seems that this operator can help us in searching for more accurate solution. It is in particular useful to fine local tuning when all chromosomes are already near each other in the population. Note that this operator may produce offspring outside the domain $\mathcal{D}$. In such a case another random value a is generated and another offspring is created. If after three attempts no new feasible solution is found, this crossover is replaced with the arithmetical crossover.

It is obvious that all three types of crossover operations are useful in the evolutional process and should be applied. But, some operators are better to use at the start of searching and some of them are more useful to use when the evolutional process finishes. Therefore we defined the probabilities of a selection for each crossover operation type in the following way:

$$p_1 = 1 - (p_2 + p_3)\,, \qquad p_1 \in (0,1) \qquad \text{for} \quad \text{simple crossover,} \tag{15}$$

$$p_2 = s_1 + s_2 s_3^{-c}, \qquad p_2 \in (0,1) \qquad \text{for} \quad \text{arithmetical crossover,} \tag{16}$$

$$p_3 = s_4 + s_5 s_6^{-c}, \qquad p_3 \in (0,1) \qquad \text{for} \quad \text{heuristic crossover,} \tag{17}$$

where $s_1, \ldots, s_6$ are chosen real parameters and $c \geq 0$. Let S_i denotes the standard deviation of numbers in the ith row of a population $P(g)$ and $\overline{\alpha_i}$ is the arithmetic mean of the same numbers. Then the parameter c is defined as

$$c = \max\left\{\left|S_1/\overline{\alpha_1}\right|, \left|S_2/\overline{\alpha_2}\right|, \ldots, \left|S_s/\overline{\alpha_s}\right|\right\}. \tag{18}$$

If the probabilities are calculated according to Eqs. (15)–(17), the selection process based on the roulette wheel is performed and the selected type of crossover is applied in the algorithm.

Note that the parameter c which means the absolute value of the variation coefficient is also used in the restart process. When the condition

$$c < \varepsilon \qquad \text{for} \quad \varepsilon > 0 \tag{19}$$

is satisfied, a new population is always generated in the evolutional process.

4.3. Mutation operation

This operator is performed on a gene-by-gene. The probability of mutation p_m provides the expected number $p_m \times P_s \times s$ of mutated genes. Every gene should have an equal chance to undergo mutation. Hence, we generate a random number r from the range $\langle 0, 1\rangle$ for each gene in the whole population. If $r < p_m$, the gene is replaced. The main purpose of mutation is to keep the variety of population in the evolutional process and allows possible movement away from a local optimum in the search for a better result. On the other hand, a frequent mutation can be the reason of a low convergence of the whole algorithm. Therefore parameter p_m is usually set less than 0.05. These are the reasons why we decided to use only a uniform mutation in our algorithm. In this case, a selected gene is replaced by a random number from the admissible domain $\mathcal{D}$.

5. In-plane shear modulus estimation

It is clear from Eqs. (4) and (7) that the FE model based on Euler-Bernoulli theory described in the section 2 is not able to identify the in-plane shear modulus G_{LT} of a cross-ply laminate. But if some fibres and matrix material properties of longitudinal composite layers are known, the modulus G_{LT} could be estimated by means of the law of mixtures [1] as presented below.

Let us consider that the values of Poisson's ratios and density of fibres and matrix are known. These parameters are usually constant for the specified material type and could be commonly found on the web site of manufacturers. Besides this, we assume that the composite material density ρ can be calculated with the aid of weight and volume of the specimen. Then the fibre volume fraction V_f can be obtained from the simplified relations expressed by

$$\rho = \rho_f\, V_f + \rho_m\, V_m \qquad \text{and} \qquad V_m = 1 - V_f\,, \tag{20}$$

where ρ_f and ρ_m are fibres and matrix density, respectively. The parameter V_m denotes matrix volume fraction. Further, we expect that the parametric optimization problem has been performed and the Young's moduli E_L and E_T were identified. If we suppose the validity of the law of mixtures for the moduli E_L and E_T, i.e.

$$E_L = E_f\, V_f + E_m\, V_m \qquad \text{and} \qquad \frac{1}{E_T} = \frac{V_f}{E_{Tf}} + \frac{V_m}{E_m}\,, \tag{21}$$

and if we define the coefficients

$$r_{mf} = \frac{E_m}{E_f} \in (0, 1\rangle\,, \qquad r_{ff} = \frac{E_f}{E_{Tf}} \geq 1 \qquad \text{and} \qquad r_{LT} = \frac{E_L}{E_T} \geq 1\,, \tag{22}$$

where E_m is matrix Young's modulus and E_f and E_{Tf} are longitudinal and transverse fibres Young's moduli, respectively, we can obtain the quadratic equation of variable r_{mf} in the form

$$(V_f\, V_m\, r_{ff})\, r_{mf}^2 + (V_f{}^2 r_{ff} + V_m{}^2 - r_{LT})\, r_{mf} + V_f\, V_m = 0\,. \tag{23}$$

Solution of this equation for the "reasonable" input coefficients r_{ff} and r_{LT} leads to finding an admissible root r_{mf} from feasible domain defined in $(22)_1$. Consequently, the relation

$$\frac{1}{G_{LT}} = \frac{V_f}{G_{LTf}} + \frac{V_m}{G_m} \tag{24}$$

is used to determine the in-plane shear modulus G_{LT}. The symbol G_{LTf} denotes the in-plane shear modulus of fibers and G_m is the shear modulus of matrix. It is concurrently assumed that these moduli could be determined for isotropic matrix material and generally orthotropic fibres material using the relations

$$G_m = \frac{E_m}{2\,(1 + \nu_m)} \qquad \text{and} \qquad G_{LTf} = \frac{E_f}{2\,(1 + \nu_f)\, r_{Gf}}\,, \tag{25}$$

where $r_{Gf} = 1$ for isotropic and $r_{Gf} > 1$ for orthotropic fibre material. The symbols ν_f and ν_m mean the major Poisson's ratio of fibres and the Poisson's ratio of matrix, respectively. By combining Eqs. $(21)_1$, $(22)_1$ and (25) with Eq. (24), we obtain

$$G_{LT} = \frac{E_L\, r_{mf}}{2\,(V_f + V_m\, r_{mf})\,[V_f\,(1 + \nu_f)\, r_{Gf}\, r_{mf} + V_m\,(1 + \nu_m)]}\,. \tag{26}$$

6. Numerical examples and discussion

Identification of elastic properties is demonstrated on examples of single-end clamped beams. These beams are assumed to be made of cross-ply laminates with various stacking sequences of layers as shown in Table 1. The geometric properties are chosen as follows: length and width of beams are 240 mm and 8 mm, respectively, each laminate has the same material properties of all layers which have the uniform thickness 0.5 mm. The mechanical properties of two investigated orthotropic composite materials are taken from [20] and are introduced in Table 2.

Table 1. Stacking sequences of used cross-ply laminates

Laminate model ID	VAR1	VAR2	VAR3
A	$[0_2/90_4/0_4]$	$[0_2/90_2/0]_S$	$[0/90]_5$
B	$[90_2/0_4/90_4]$	$[90_2/0_2/90]_S$	$[90/0]_5$

Table 2. Mechanical properties of used unidirectional laminae

Composite material type	T300/BSL914C epoxy	E-Glass/MY750/HY917/DY063 epoxy
Material model ID	MAT1	MAT2
Fibre volume fraction, V_f $[-]$	0.6	0.6
Longitudinal modulus, E_L [GPa]	138	45.6
Transverse modulus, E_T [GPa]	11	16.2
Shear modulus, G_{LT} [GPa]	5.5	5.83
Major Poisson's ratio, ν_{LT} $[-]$	0.28	0.278
Transverse Poisson's ratio, $\nu_{TT'}$ $[-]$	0.4	0.4

The vector $\mathbf{\Omega}^{\exp}$ of frequencies is not stated experimentally but is calculated numerically with the help of software MSC.Marc. This approach was chosen to verify the quality of the material identification process when the FE model with beam elements described in this work has been employed. At first, we analyzed the influence of the number of used FEs on values of first four flexural frequencies. The mesh of 32×2 regular four-node isoparametric shell elements with linear approximations of displacements was created using the software of MSC.Mentat. On the contrary, the beam element model contained only 8 elements. It was observed that the increase of element number in both model has a very small influence on the change of flexural eigenfrequencies values. As shown in Table 3 for laminate model VAR1, the eigenfrequency errors are about $5\,\%$ in comparison to both numerical model results. We came to similar conclusions in all other calculated cases.

Table 3. First four flexural frequencies in cycles per time, laminate model VAR1

FE model	ID	MAT1				MAT2			
		1	2	3	4	1	2	3	4
Shell elements (MSC.Marc)	A	124.2	770.4	2124	4073	63.54	397.5	1111	2171
	B	51.01	319.5	894.7	1754	42.72	267.8	750.5	1474
Beam elements	A	124.9	782.2	2190	4292	64.66	405.1	1134	2223
	B	53.64	336.0	940.5	1844	45.94	287.7	805.5	1579

The identification process of elastic Young's moduli and the major Poisson's ratio was performed according to optimization problem (11). However, it could happen that the same eigenfrequencies $\boldsymbol{\Omega}(\boldsymbol{p})$ can be obtained from different values of input material parameters $\boldsymbol{p} = [E_L, E_T, \nu_{LT}]^T$ because the beam is made from orthotropic layers of a various orientation. Therefore, the objective function $f(\boldsymbol{p})$ in Eq. (11) is constructed as a weighted sum of functions

$$f(\boldsymbol{p}) = \xi_1 \, f_A(\boldsymbol{p}) + \xi_2 \, f_B(\boldsymbol{p}) \,, \qquad \xi_1 = 1 \,, \quad \xi_2 = 1 \,, \tag{27}$$

while the same material model ID is assumed. The indexes A and B mean various layer sequences stated in the columns of Table 1. This modification of objective function should lead to the unique solution of elastic parameters. Only first four flexural eigenfrequencies for every variant A and B are accepted in the whole optimization process. This limit is set for the reason of ability to reliably detect their maximum values in experimental way in the future.

The GA and the μGA were used to solve the optimization problem (11) where the objective function was constructed according to (27). The tournament selection and elitism were applied in all presented simulations. The restart process with parameter $\varepsilon = 0.001$ was also active in all calculations. The crossover and the mutation probabilities were set to be equal to 0.95 and 0.05, respectively, in the case of GA. When the μGA was employed, the crossover operation was used with the same probability but the mutation operation was omitted. The parameters in Eqs. (16) and (17) which have influence on the selection of the crossover operation type were chosen as follows: $s_1 = 0.3$, $s_2 = 0.1$, $s_4 = 0.2$, $s_5 = 0.3$ and $s_3 = s_6 = 1 \cdot 10^6$. The maximum number of generated chromosomes during the process was invariable and was set equal to 3000. Furthermore, every optimization problem was independently repeated 50 times and the obtained results were evaluated statistically.

Table 4. Statistical evaluation of E_L [GPa] and E_T [GPa], laminate model VAR1

$P_s \cdot N_g$	MAT1				MAT2			
	E_L^a	S_{E_L}	E_T^a	S_{E_T}	E_L^a	S_{E_L}	E_T^a	S_{E_T}
100·30	131.3	0.415	9.609	0.012	44.52	0.548	13.70	0.008
60·50	131.3	0.519	9.612	0.029	44.49	0.594	13.71	0.026
30·100	130.7	2.691	9.634	0.149	44.21	1.247	13.73	0.129
6·500	131.3	0.612	9.605	0.014	44.22	0.817	13.71	0.028

The identification process was started for the following estimation intervals of unknown material parameters: $E_L \in \langle 10, 1000 \rangle$ [GPa], $E_T \in \langle 1, 100 \rangle$ [GPa], $\nu_{LT} \in \langle 0.1, 0.4 \rangle$ $[-]$. It can be seen from Table 4 for the case of laminate model VAR1 that the average values of longitudinal modulus E_L^a and transverse modulus E_T^a give very similar results for various population size P_s. The results in the last row of Table 4 were obtained by using the μGA whereas the others by using the GA. The average estimations of the longitudinal modulus for MAT1 and MAT2 were different about $5\,\%$ from expected values in Table 2. But the errors about $15\,\%$ (difference of 2.5 GPa between real and calculated values) were detected for the transverse moduli. Besides, it can be concluded from Table 4 that the robustness of the GA and the μGA in regard to choice of initial Young's moduli values is very good because the standard deviations S_{E_L} and S_{E_T} are small in comparison to average values of E_L^a and E_T^a. Much worse results were obtained in the Poisson's ratio calculation. As shown in Table 5, determined average Poisson's ratios ν_{LT}^a are not near to expected values of this parameter, even though the best Poisson's ratios ν_{LT}^b are rather close to the real values given in Table 2. It is obvious that the identification problem has

Table 5. Statistical evaluation of ν_{LT} $[-]$, laminate model VAR1

$P_s \cdot N_g$	MAT1			MAT2		
	ν_{LT}^b	ν_{LT}^a	S_ν	ν_{LT}^b	ν_{LT}^a	S_ν
100·30	0.281	0.241	0.068	0.286	0.239	0.078
60·50	0.281	0.245	0.087	0.277	0.242	0.080
30·100	0.282	0.263	0.118	0.276	0.252	0.106
6·500	0.266	0.233	0.105	0.276	0.270	0.101

a small sensitivity in relation to this parameter, which can be shown by means of the standard deviation S_ν in Table 5, because the ratios of S_ν to ν_{LT}^a give relatively large values against to coefficients of variation S_{E_L}/E_L^a and S_{E_T}/E_T^a. However, the value of the Poisson's ratio can be usually found in a local range for specified material type and it can be estimated reliable using the law of mixtures

$$\nu_{LT} = \nu_f V_f + \nu_m V_m \,. \tag{28}$$

In view of the fact that similar results were also obtained in the case of the laminate model VAR2 and VAR3, the Poisson's ratio ν_{LT} has been next calculated according to Eq. (28) and was removed from a vector of unknown parameters $\boldsymbol{p}$. The value of ν_{LT} is then equal to 0.26 for both material models MAT1 and MAT2 while the Poisson's ratios of fibres and matrix have been adopted from [20], see Tables 6 and 7. Differences of computed and real (Table 2) values are less than $7\,\%$.

Table 6. Mechanical properties of used fibres

Fibre type	T300	Silenka E-Glass 1200tex
Longitudinal modulus, E_f [GPa]	230	74
Transverse modulus, E_{Tf} [GPa]	15	74
In-plane shear modulus, G_{LTf} [GPa]	15	30.8
Transverse shear modulus, $G_{TT'f}$ [GPa]	7.0	30.8
Major Poisson's ratio, ν_f $[-]$	0.2	0.2

Table 7. Mechanical properties of used matrices

Matrix type	BSL914C epoxy	MY750/HY917/DY063 epoxy
Modulus, E_m [GPa]	4.0	3.35
Shear modulus, G_m [GPa]	1.48	1.24
Poisson's ratio, ν_m $[-]$	0.35	0.35

The identification process has been repeated again to generate a new vector of unknown material parameters $\boldsymbol{p} = [E_L, E_T]^T$. The Poisson's ratio ν_{LT} was assumed constant during every computation and equals to 0.26 for all laminate and material models. The longitudinal and transverse moduli obtained using the μGA and the GA for various numbers of P_s and N_g gave very similar results. Therefore, only the results of the μGA are presented in the following text. The ranges of investigated parameters were chosen as above, i.e. $E_L \in \langle 10, 1000\rangle$ [GPa], $E_T \in \langle 1, 100\rangle$ [GPa].

As it is obvious from Tables 8 and 9 for VAR1 and VAR2, the value of the Poisson's ratio ν_{LT} has a neglected influence on computation of Young's moduli E_L and E_T in comparison to results in Table 4. The low values of the standard deviations S_{E_L} and S_{E_T} mean that our optimization algorithm is robust for searching parameters. However, these conclusions are not

Table 8. Statistical evaluation of longitudinal modulus E_L [GPa], $\nu_{LT} = 0.26$ [−]

Model	MAT1			MAT2		
	VAR1	VAR2	VAR3	VAR1	VAR2	VAR3
E_L^b	131.7	131.9	137.5	44.53	44.80	45.52
E_L^a	131.3	131.6	95.29	44.46	44.57	27.97
S_{E_L}	0.109	0.148	35.40	0.033	0.079	15.19

Table 9. Statistical evaluation of transverse modulus E_T [GPa], $\nu_{LT} = 0.26$ [−]

Model	MAT1			MAT2		
	VAR1	VAR2	VAR3	VAR1	VAR2	VAR3
E_T^b	9.619	10.43	11.00	13.72	13.88	15.65
E_T^a	9.606	10.30	38.64	13.71	13.77	26.83
S_{E_T}	0.006	0.037	27.03	0.005	0.029	11.73

valid in the case of VAR3 because incorrect results were obtained for average Young's moduli. In addition, large values of standard deviation were computed. The reason of errors lies in the unsuitable assemblage of composite layers, see Table 1. The laminate model VAR3 can be taken into account as quasi-isotropic on a macroscopic scale in both variants A and B. Therefore, the vector of computed eigenfrequencies is the same in variant A and B. Due to this fact, there is not only one solution of the optimization problem in the domain $\mathcal{D}$. This conclusion follows from the very low objective function value at the end of the optimization process when the number of generated chromosomes is equal to $3\,000$. This occurrence was observed in all considered cases.

It was discussed in the section 5 that the presented mathematical model of the beam is not able to identify the in-plane shear modulus G_{LT}. Therefore, the method of this modulus estimation has been proposed. The calculations of G_{LT} were performed for the average Young's moduli given in Tables 8 and 9, and for the Poisson's ratios given in Tables 6 and 7. The coefficients r_{ff} and r_{Gf} were set according to elastic moduli values of fibers in Table 6. While E-glass fibers have isotropic properties and due to the both coefficients were set equal to 1, T300 carbon fibres are orthotropic and the coefficients were determined as follows: $r_{ff} = 230/15 \doteq 15.3$, see Eq. $(22)_2$; $G_{LTf} \equiv E_{Tf} \Longrightarrow r_{Gf} = r_{ff}/[2\,(1+\nu_f)] = 15.3/[2\,(1+0.2)] \doteq 6.39$, see Eqs. $(22)_2$ and $(25)_2$. The volume fraction $V_f = 0.6$ (Table 2) was assumed constant in all calculated problems. Note that the mechanical properties of a certain material class, as Young's moduli or the Poisson's ratio, are usually almost invariable. This fact can be also supported for the carbon fibres (namely for fibre types AS4 and T300) by experimental data given in [20]. Therefore, we can suggest the set of coefficients $r_{ff} = 15$ and $r_{Gf} = 6.2 \div 6.4$ when the specific material properties of the carbon fibres are unknown.

The results of G_{LT} calculations for VAR1 and VAR2 are stated in Table 10. The variant VAR3 was not considered. When we compare the values of shear modulus from Tables 2 and 10 it is evident that the best computed value was found in the case of the material model MAT1 and VAR2 where the relative error was less than $4\,\%$. In the rest cases, the relative difference between the known and calculated values is about $12\,\%$, which is result comparable to results obtained for the transverse moduli. If we compute the shear modulus G_{LT} only with real data from Tables 2, 6 and 7, we obtain even more better results. These moduli are as follows: $G_{LT} = 5.69$ [GPa] for MAT1 (error $3.4\,\%$) and $G_{LT} = 6.09$ [GPa] for MAT2 (error $4.5\,\%$).

Table 10. Calculated values of average shear modulus G_{LT} [GPa], $V_f = 0.6$ [−]

Model	MAT1		MAT2	
	VAR1	VAR2	VAR1	VAR2
r_{LT}	13.67	12.78	3.243	3.237
r_{mf}	0.030	0.034	0.088	0.089
G_{LT}	4.804	5.286	5.145	5.168

7. Conclusion

It has been shown in this paper that the robustness of genetic algorithms is very good for the determination of Young's moduli values. This method is particularly effective for a low time-consuming computation of chromosomes in a generation. Acceptable values of the modulus E_L were calculated but worse results were obtained for moduli E_T and G_{LT}. These results are partially influenced by the selection of used mathematical model of a beam because of the differences between eigenfrequencies obtained from shell and beam elements. The calculation of the shear modulus G_{LT} was then directly dependent on the values of E_L and E_T. The computation of the Poisson's ratio ν_{LT} gave high standard deviation values when inverse procedure was used for identification. However, a small influence of ν_{LT} value on values of Young's moduli was found. In practice the value of ν_{LT} is quite close in vicinity of 0.3 and can be stayed close to this value or can be computed by using the law of mixtures when the volume fraction of fibers and the Poisson's ratios of the fibers and the matrix are known.

The proposed methodology has some disadvantages. The measurement of eigenfrequencies has to be performed on two independent specimens with different layer sequences. Due to this fact, the beam specimen made of a quasi-isotropic laminate is not suitable to use for the identification of material properties. In addition, we have to determine the volume fraction of fibers and we have to know some material properties of fibers and matrix when we want to apply the law of mixtures in the calculation of ν_{LT} and G_{LT}. It requires the knowledge of fibers and matrix material properties. On the other hand, the proposed methodology brings some advantages. The method enables to utilize the simple specimens. Mechanical properties are directly calculated for a final laminate. Only a few eigenfrequencies given by the simple test are needed to be computed values of Young's moduli E_L and E_T. The required measuring aparatures are not as expensive as typical static testing machines.

In future, the real measuring of eigenfrequencies is prepared and different mathematical model of the beam which gives higher accuracy of calculated frequencies should be used.

Acknowledgements

This work has been supported by the European project NTIS-New Technologies for Information Society No.: CZ.1.05/1.1.00/02.0090.

References

[1] Altenbach, H., Altenbach, J., Kissing, W., Mechanics of composite structural elements, Springer, Berlin, 2004.

[2] Balasubramaniam, K., Rao, N. S., Inversion of composite material elastic constants from ultrasonic bulk wave phase velocity data using genetic algorithms, Composites 29 B (1998) 171–180.

[3] Chang, W. D., Nonlinear system identification and control using a real-coded genetic algorithm, Applied Mathematical Modelling 31 (2007) 541–550.

[4] Chen, C. M., Kam, T. Y., A two-level optimization procedure for material characterization of composites using two symmetric angle-ply beams, International Journal of Mechanical Sciences 49 (2007) 1 113–1 121.

[5] Chu, Y. C., Rokhlin, S. I., Stability of determination of composite moduli from velocity data in planes of symmetry for weak and strong anisotropies, Journal of the Acoustical Society of America 95 (1) (1994) 213–225.

[6] Frederiksen, P. S., Application of an improved model for the identification of material parameters, Mechanics of Composite Materials and Structures 4 (4) (1997) 297–316.

[7] Genovese, K., Lamberti, L., Pappalettere, C., A new hybrid technique for in-plane characterization of orthotropic materials, Experimental Mechanics 44 (6) (2004) 584–592.

[8] Goldberg, D. E., Genetic algorithms in search, optimization and machine learning, Addison-Wesley, Boston, 1989.

[9] Han, X., Liu, G. R., Li, G. Y., Transient response in cross-ply laminated cylinders and its application to reconstruction of elastic constants, Computers, Materials and Continua 1 (1) (2004) 39–49.

[10] Ip, K. H., Tse, P. CH., Lai, T. CH., Material characterization for orthotropic shells using modal analysis and Rayleigh-Ritz models, Composites 29 B (1998) 397–409.

[11] Kam, T. Y., Liu, C. K., Stiffness identification of laminated composite shafts, International Journal of Mechanical Sciences 40 (9) (1998) 927–936.

[12] Lecompte, D., Smits, A., Sol, H., Vantomme, J., Van Hemelrijck, D., Mixed numerical-experimental technique for orthotropic parameter identification using biaxial tensile tests on cruciform specimen, International Journal of Solids and Structures 44 (2007) 1 643–1 656.

[13] Liu, G. R., Han, X., Lam, K. Y., A combined genetic algorithm and nonlinear least squares method for material characterization using elastic waves, Computer Methods in Applied Mechanics and Engineering 191 (2002) 1 909–1 921.

[14] Liu, G. R., Ma, W. B., Han, X., An inverse procedure for determination of material constants of composite laminates using elastic waves, Computer Methods in Applied Mechanics and Engineering 191 (2002) 3 543–3 554.

[15] Liu, G. R., Tani, J., Ohyoshi, T., Watanabe, K., Transient waves in anisotropic laminated plates, Journal of Vibration and Acoustics 113 (1) (1991) 230–239.

[16] Liu, G. R., Xi, Z. C., Elastic waves in anisotropic laminates, CRC Press LLC, Boca Raton, 2002.

[17] Michalewicz, Z., Genetic algorithms + data structures = evolution programs, Springer, Berlin, 1995.

[18] Mota Soares, C. M., de Freitas, M. M., Araújo, A. L., Pedersen, P., Identification of material properties of composite plate specimens, Composite Structures 25 (2) (1993) 277–285.

[19] Rikards, R., Chate, A., Steinchen, W., Kessler, A., Bledzki, A. K., Method for identification of elastic properties of laminates based on experiment design, Composites 30 B (1999) 279–289.

[20] Soden, P. D., Hinton, M. J., Kaddour, A. S., Lamina properties lay-up configurations and loading conditions for range of fibre-reinforced composite laminates, Composites Science and Technology 58 (1998) 1 011–1 022.

[21] Wang, L., Tang, F., Wu, H., Hybrid genetic algorithm based on quantum computing for numerical optimization and parameter estimation, Appl. Math. Comput. 171 (2005) 1 141–1 156.

[22] Zajíček, M., Adámek, V., Dupal, J., Finite element for non-stationary problems of viscoelastic orthotropic beams, Applied and Computational Mechanics 5 (1) (2011) 89–100.